Original Article

Imaging analysis for multiple paramagnetic agents using OMRI and electrophoresis

Ayano Enomoto,[1] Nao Kato,[2] Naomi Shirouzu,[2] Chihiro Tamura,[2] and Kazuhiro Ichikawa[1,2,3,*]

[1]Department of Biophysical Chemistry, Faculty of Pharmaceutical Sciences, Nagasaki International University, 2825-7 Huis Ten Bosch, Sasebo, Nagasaki 859-3298, Japan
[2]Innovation Center for Medical Redox Navigation and [3]Incubation Center for Advanced Medical Science, Kyushu University, 3-1-1 Maidashi, Higashi-ku, Fukuoka, Fukuoka 812-8582, Japan

(Received 19 October, 2020; Accepted 5 July, 2021; Released online in J-STAGE as advance publication 25 September, 2021)

Nitroxides have been widely used as a molecular probe for analysis of various diseases models. This article describes an analytical method for separation and semi-quantification of multiple paramagnetic contrast agents with simple procedure combining electrophoresis and Overhauser enhancement magnetic resonance imaging (OMRI) imaging. We used three nitroxides, 3-carbamoyl PROXYL, 3-carboxy PROXYL, and CAT-1, which have different ionic charges in the molecule. In addition, we showed that this method could apply for *in vitro* measurement using biological sample. The results showed the nitroxides were successfully separated with electrophoresis depending on their charge, and their separation was visualized with OMRI after electrophoresis. Vehicle media such as whole blood did not affect the electrophoresis results and OMRI enhancement factor. Thus, the method can be used to analyze the redox status of biological samples without preprocessing. This analytical method enables *in vitro* measurement of biological samples to determine the redox status of specific tissue layers using paramagnetic agents, which is helpful for detailed analysis of redox-related diseases.

***Key Words*: separation and analysis, multiple paramagnetic agents, Overhauser enhanced MRI, electron paramagnetic resonance**

Free radicals including reactive oxygen species and reactive nitrogen species are associated with various physiological processes such as immune functions[1] and cellular signaling.[2] Excess production of reactive oxygen species causes disorders in the redox balance and oxidative damage to cells and tissues,[3] resulting in the onset of various diseases such as ischemia reperfusion,[4,5] inflammation,[6] and diabetes.[7,8]

Monitoring of the redox status *in vivo* would be useful for investigating the pathology of diseases related to oxidative stress. Electron paramagnetic resonance (EPR) or Overhauser enhancement MRI (OMRI) are frequently used for imaging of the redox status in the animal body.[7–9] These methods utilize molecular probes containing paramagnetic sites, such as nitroxides, as "spin probes".[10]

Nitroxides can be used to investigate the redox status because they have moderate stability and reactivity with redox-reactive substances, such as ROS, RNS, antioxidants, and reducing equivalent such as TEMPOL.[11,12] The antioxidant effects of nitroxides[13] in animal disease models are reported to depend on the octanol/water distribution coefficients.[14] For example, nitroxide compounds act as antioxidants and have different mechanisms to inhibit gastric ulcers depending on their properties.[14,15] Two spin probes, which were either membrane-permeable or membrane-impermeable probes were also detected simultaneously in the intra- and extracellular compartments of the stomach of rats with indomethacin-induced gastric ulcers and the difference in the suppression of gastric mucosal damage was investigated using a live rat stomach with indomethacin-induced gastric ulcers.[15] As reported in those papers, observing nitroxides with different tissue permeability is important to know point of action of each nitroxide in gastric mucosa and also useful to understand the detail mechanism of ulcer formation. Therefore, by using multiple nitroxides with different tissue permeability, detailed analysis of nitroxides reduction distributed in different layers of gastric mucosal would be possible and be utilized to know the more detail mechanism of gastric diseases related to free radicals.

However, simultaneous detection of more than two spin probes in *in vivo* have not achieved because there were no methods to detect more than two nitroxides simultaneously. There are some reports describing methods for assessing two nitroxides simultaneously with EPR[16] or OMRI.[17,18] These studies utilized two nitroxides either with ^{14}N or ^{15}N nitrogen, which gives a different paramagnetic spectrum, enabling simultaneous measurement by OMRI or EPR. However, isotopic labeling method is limited to the number of stable isotopes of each nuclide to detect multiple agents. In case of nitroxide, there are only two stable isotopes of nitrogen.

The current study was conducted to demonstrate the feasibility of a new analysis method using OMRI and electrophoresis to separate and image more than two nitroxides simultaneously. We focused on the electric charge of nitroxides, demonstrating that three nitroxides were separated by electrophoresis and semi-quantified by an OMRI system, which is appropriate for detecting small amounts of free radical samples because of its high sensitivity.

Materials and Methods

Chemicals. Three nitroxides were used in the study; negatively charged 3-carboxy-PROXYL (CxP; Sigma Aldrich, St. Louis, MO), neutral charged 3-carbamoyl-PROXYL (CmP; Sigma Aldrich), and positively charged 1-oxy-4-trimethylamine-2,2,6,6,tetramethyl-piperidine (CAT-1; Invitrogen, Carlsbad, CA). These nitroxides are selected since they are frequently used for *in vivo* measurement.[8,19,20]

Measurement of 9.4-GHz EPR spectra. In OMRI, because the NMR signal intensity of the area in which free radicals were distributed is amplified as a result of the transfer of polarization from electrons to protons, EPR irradiation at an appropriate microwave (MW) frequency was required to obtain the distribu-

*To whom correspondence should be addressed.
E-mail: ichikawak@niu.ac.jp

doi: 10.3164/jcbn.20-172

tion image of nitroxides. Therefore, to verify the EPR absorption positions of CxP, CmP, and CAT-1, we obtained their 9.4-GHz X-band EPR spectra. X-band EPR spectra were obtained to verify the EPR absorption position of 4 mM aqueous solution of nitroxides using an X-band EPR spectrometer (JES-RE01; JEOL, Tokyo, Japan).

Additionally, to determine the optimum concentration of nitroxides, we investigated the relation between the concentration and EPR signal intensity.

The parameters were as follows: 9.4 GHz microwave frequency, 330.8 mT center field, 10 mT scanning field, 8,192 acquisition points, 0.1 mT magnetic field modulation, 100 kHz modulation frequency, 120 s field scanning duration, 0.3 s time constant, and 1 mW incident power. The absorption position was calculated using the middle peak of the triplet EPR signal. Calibration curves were obtained using 0.5, 1, 2, 3, 4, and 5 mM aqueous solutions of nitroxides. The number of each nitroxide was calculated by double integration of each EPR spectrum.

Electrophoresis of nitroxides. To demonstrate that sample included multiple nitroxides were separated with electrophoresis method, we mixed an equal volume of 12 mM solutions of the three nitroxides to prepare a mixed solution containing 4 mM of each nitroxide. We compared the three individual nitroxide solutions and mixture solution.

Furthermore, to investigate the effect of using biological samples on the electrophoresis of nitroxides, we mixed each nitroxide with serum or whole blood from mice. Blood samples were obtained approximately 500–1,000 µl from 5–7-week-old female C57BL mouse (CLEA JAPAN, Inc., Tokyo, Japan). The serum was prepared using a standard method. Whole blood samples were mixed with the individual nitroxides immediately after blood sampling. To prepare biological samples containing nitroxide, we mixed equal amount of 8 mM nitroxide aqueous solution and the serum or whole blood to give a final nitroxide concentration of 4 mM. All procedures involving animals were approved by the ethics committee of Nagasaki International University.

For gel electrophoresis, 1% agarose gel (FUJIFILM Wako Pure Chemical Corporation, Osaka, Japan) was prepared with Tris-acetate EDTA buffer (FUJIFILM Wako Pure Chemical Corporation). The size of each well was 2 × 3 × 7.5 mm and the gap between wells was 2 mm. Before starting electrophoresis, the agarose gel was left in Tris-acetate EDTA buffer for at least 10 min, after which 30-µl samples were applied to each well as shown in Fig. 3A. For a set of one measurement, a mixture of nitroxides, CAT-1, CmP, and CxP was applied to the gel (Fig. 3A).

Electrophoresis was performed at a constant voltage of 135 V for 7 min, and then a gel piece 22 × 25 × 9 mm was cut from the gel to fit an OMRI measurement tray (25 mm × 30 mm × 9 mm). All experiments were carried out 4 times.

OMRI imaging. A laboratory-built 16 mT OMRI system was used in the experiments. For EPR excitation, a 30 × 30 mm square surface coil resonator was used (Supplemental Fig. 1A*). After electrophoresis, a gel piece in the OMRI measurement tray was placed in the slot of the EPR surface coil to assure reproduction in repeatable measurements (Supplemental Fig. 1B*). The NMR frequency was 685 kHz and EPR excitation frequency was set to 456 MHz. The parameters for OMRI were as follows: 1,000 ms repetition time, 40 ms echo time, 60° flip angle, 500 ms EPR excitation time, 60 × 60 mm field of view, 0.93 × 0.93 mm pixel size, 100 mm slice thickness, and 9 accumulation times.

To calculate the enhancement factor, we used a mean value of 3 × 4 pixels (2.8 × 3.7 mm) to completely cover the individual area of the wells, considering that OMRI images were blurred because of diffusion during electrophoresis. The enhancement factor was calculated as the ratio of the mean values of signal intensity of the well area including each nitroxide to those of the same position in the image without EPR excitation. The enhancement factors were evaluated by analysis of variance.

Results

Comparison of absorption position of nitroxides. Figure 1 shows the comparison of the spectra of each nitroxide. To investigate details of spectra, we magnified the middle peak of

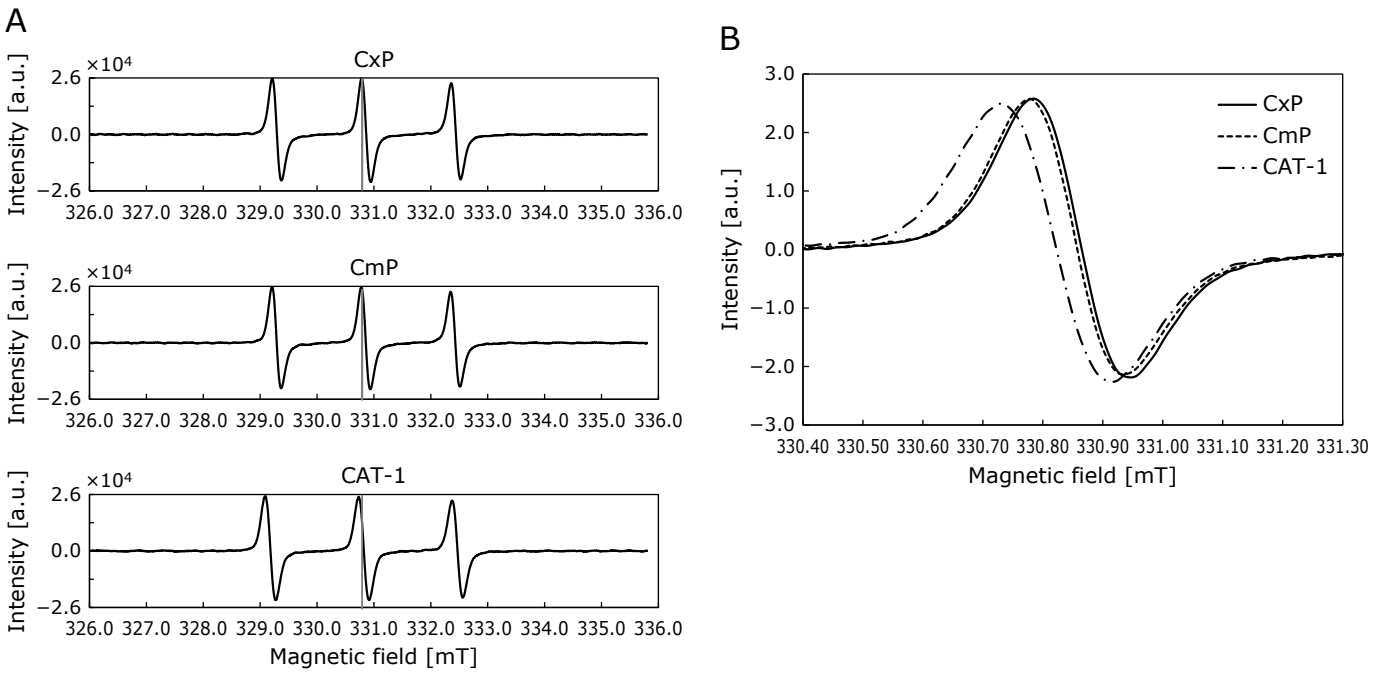

Fig. 1. Comparison of 9.4-GHz EPR spectra and concentration dependence of 4 mM CxP, CmP, and CAT-1. (A) Comparison of triplet EPR spectra of nitroxides. (B) Magnified view of middle peaks of three nitroxides shown in (A).

*See online. https://doi.org/10.3164/jcbn.20-172

doi: 10.3164/jcbn.20-172

the spectra shown in Fig. 1A. As shown in Fig. 1B, the zero crossing points of the middle peaks of CxP, CmP, and CAT-1 were 330.87, 330.86, and 330.82 mT, respectively. The maximum difference in the absorption point was 0.05 mT (CxP and CAT-1), i.e., approximately 1 MHz difference in the EPR frequency at X-band.

Relation between concentration and EPR signal intensity. The EPR signal intensity was proportional to the concentrations of nitroxides up to 4 mM (Fig. 2). As the initial blood concentration of nitroxides is generally 4–10 mM in animal experiments, a concentration of 4 mM nitroxides is reasonable for all experiments including animal experiments and thus was used for semi-quantification analysis.

Visualization of nitroxides in gel. We separated the nitroxide mixture based on charge by electrophoresis and then visualized the separated nitroxides by OMRI. Figure 3 shows the results of gel OMRI before and after electrophoresis. As shown in Fig. 3A, it was difficult to identify individual nitroxide from a mixture without electrophoresis. In contrast, as shown in Fig. 3B–D, the nitroxide mixture was separated based on the charge of each nitroxide by electrophoresis. The distance moved by charged nitroxides (CxP or CAT-1) in the mixture was similar to the distance moved by those in single nitroxide aqueous solutions. Figure 3C and D show the results of gel imaging of nitroxides in a biological sample. Although there were some differences in the distance moved, each nitroxide could be identified and semi-quantified after electrophoresis. Table 1 shows the comparison of enhancement factor of each nitroxides in different vehicle media. As a result of analysis of variance, p value were 0.10 for CAT-1, 0.34 for CmP and 0.13 for CxP, respectively. There was no significant difference depending on vehicle media.

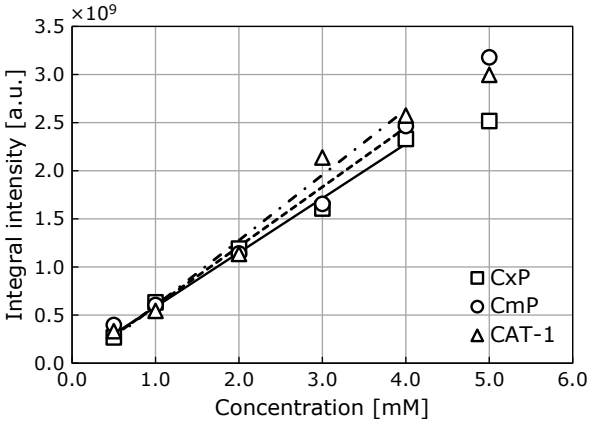

Fig. 2. EPR double integral intensity versus concentration for CxP, CmP, and CAT-1. When the concentrations were less than 4 mM, EPR double integral intensity was proportional to the concentration of CxP, CmP, and CAT-1 and the correlation coefficients (r^2 values) were 0.97, 0.99, and 0.97, respectively.

Discussion

The experimental results indicate that separation and semi-quantification of individual nitroxides in a mixture was possible by combining electrophoresis with OMRI. Therefore, since vehicle media such as whole blood did not affect the electrophoresis results (Fig. 3C and D) or OMRI enhancement factor (Table 1), the method can be used to analyze the redox status of biological samples without preprocessing.

Variations in OMRI enhancement among nitroxides depend on multiple factors. The average enhancement factor of CmP was approximately 2-fold higher than that of CxP and CAT-1, as shown in Table 1. According to dynamic nuclear polarization theory,[21] the lineshape of the spectra of nitroxides, i.e., electron

Table 1. The enhancement factor when the different solvent was applied

	In water	In serum	In whole blood
CAT-1	2.17 ± 0.09	2.73 ± 0.48	1.88 ± 0.18
CmP	4.53 ± 0.13	5.02 ± 1.60	4.11 ± 0.29
CxP	2.44 ± 0.40	2.08 ± 0.34	1.64 ± 0.03

The enhancement factor was calculated with the methods referred in Materials and Methods. Values are means ± SD of each three measurements.

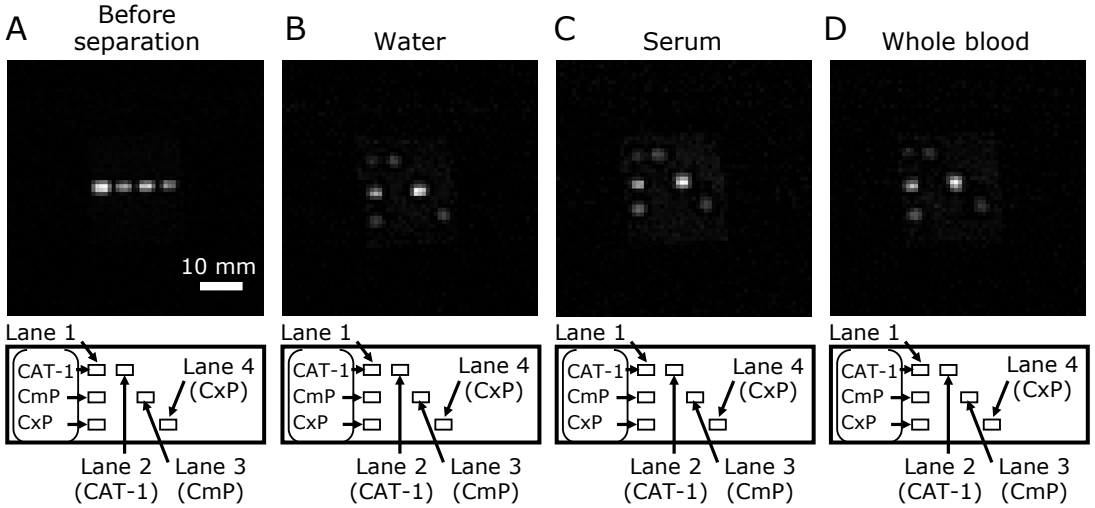

Fig. 3. Gel electrophoresis results of CxP, CmP, and CAT-1, and the mixture of these three free radical reagents. OMRI images were obtained (A) without electrophoresis, Lane 1: mixture of CxP, CmP, and CAT-1, Lane 2: CAT-1, Lane 3: CmP, Lane 4: CxP, or after electrophoresis with a vehicle media of (B) distilled water; (C) serum; and (D) whole blood, respectively. Experimental parameters for electrophoresis and OMRI measurement are described in the Methods.

relaxation, is one factor related to the degree of EPR saturation. The linewidths of each nitroxide calculated from Fig. 1B were 0.164, 0.156, and 0.184 mT for CxP, CmP, and CAT-1, respectively. The order of the linewidth was inversely correlated with that of the enhancement factors of the nitroxides.

The response of each nitroxide to the MW frequency for EPR excitation also could contribute to the difference in the enhancement factor (Fig. 1B). Although each nitroxide had optimum exciting frequency, the differences in MW frequency for EPR excitation were approximately 40 kHz at 15 mT and may cause small effect on enhancement factors as shown in Supplemental Fig. 2*. Thus, we decided to use single frequency for EPR excitation.

The other reason for the difference in the enhancement factor may be the inhomogeneity of the B_1 field generated by the EPR excitation coil. As shown in Supplemental Fig. 2*, because the difference of enhancement factors was within the measurement error when nitroxide aqueous samples were placed the same position, B_1 field distribution would affect variations in OMRI enhancement between each nitroxide shown in Table 1. The bands of CAT-1 and CxP after electrophoresis were approximately 6 and 7 mm away from the wells (Supplemental Fig. 1B* and Fig. 3B–D). Therefore, the B_1 field intensity may be lower than that at the center of the coil, at which CmP remained, and may contribute to smaller enhancement factors. Further, as shown in Fig. 3A, as the nitroxide mixture in lane 1 was placed on the edge of the coil, the enhancement factors appeared to be lower than that in the other lane. The compensation for the B_1 distribution should be determined in future studies for nitroxide quantification.

We separated and analyzed individual nitroxides from a nitroxide mixture by combining electrophoresis and OMRI, although some technical issues must be overcome. One difficulty of this method is extending the homogenate B_1 area to measure more than three probes. Because the size of the gel used for electrophoresis would be increased as additional probes are used, the B_1 homogeneous area was limited. A larger coil or array coil can expand the B_1 area.[22] The EPR excitation of each nitroxide must also be optimized. It would be helpful to switch the MW frequency to the corresponding optimal EPR frequency of each nitroxide to improve the enhancement factor and quantification of nitroxides.

In theory, the number of nitroxide probes can be increased if there are differences in the ionic valences of the probes. Therefore, for *in vitro* measurements, compared to isotopic labeling, our method is practical for investigating the redox status in living animals because more than two reagents can be used in this simple process.

Conclusion

We demonstrated the feasibility of an analytical method for separating and imaging multiple nitroxides simultaneously using electrophoresis and OMRI. Depending on the moieties of nitroxides, CmP, CxP, and CAT-1 were successfully separated and imaged in a mixture after electrophoresis and OMRI. This method is applicable for *in vitro* measurement of biological samples. In principle, this method can separate more than three paramagnetic compounds based on the ion valence. This approach can be utilized for *in vitro* analysis of multiple probes, which may be useful for detailed investigation of the redox status in specific tissue layers.

Acknowledgments

This work was in part supported by JSPS KAKENHI [Grant numbers 15H03035, 26560215, 18K19381 (KI)] and the funding program ‘Creation of Innovation Centers for Advanced Interdisciplinary Research Areas’ from JST; JSPS KAKENHI [Grant numbers 19K21118 and 18H05964 (AE)]. In addition, we would like to thank Editage for English language editing.

Abbreviations

CAT-1	1-oxy-4-trimethylamine-2,2,6,6,tetramethyl-piperidine
CmP	3-carbamoyl-2,2,5,5-tetramethylpyrrolidin-1-yloxy
CxP	3-carboxy-2,2,5,5-tetramethyl-1-pyrrolidinyloxy

Conflict of Interest

No potential conflicts of interest were disclosed.

References

1 Wink DA, Hines HB, Cheng RYS, *et al*. Nitric oxide and redox mechanisms in the immune response. *J Leukoc Biol* 2011; **89**: 873–891.
2 Klotz L-O, Briviba K, Sies H. 1 - Signaling by singlet oxygen in biological systems. In: Sen CK, Sies H, Baeuerle PA, eds. *Antioxidant and Redox Regulation of Genes*. San Diego: Academic Press, 2000; 3–20.
3 Sies H, Jones D. Oxidative stress. In: Fink G, ed. *Encyclopedia of Stress*, Cambridge: Academic Press, 2007; 45–48.
4 Kuppusamy P, Zweier JL. Cardiac applications of EPR imaging. *NMR Biomed* 2004; **17**: 226–239.
5 Zweier JL, Talukder MAH. The role of oxidants and free radicals in reperfusion injury. *Cardiovasc Res* 2006; **70**: 181–190.
6 Yamada K, Nakamura T, Utsumi H. Enhanced intraarticular free radical reactions in adjuvant arthritis rats. *Free Radic Res* 2006; **40**: 455–460.
7 Inoguchi T, Li P, Umeda F, *et al*. High glucose level and free fatty acid stimulate protein kinase C—dependent activation of NAD(P)H oxidase in cultured vascular cells. *Diabetes* 2000; **49**: 1939–1945.
8 Sano T, Umeda F, Hashimoto T, Nawata H, Utsumi H. Oxidative stress measurement by *in vivo* electron spin resonance spectroscopy in rats with streptozotocin-induced diabetes. *Diabetologia* 1998; **41**: 1355–1360.
9 Kishimoto S, Krishna MC, Khramtsov VV, Utsumi H, Lurie DJ. *In vivo* application of proton-electron double-resonance imaging. *Antioxid Redox Signal* 2018; **28**: 1345–1364.
10 Caia GL, Efimova OV, Velayutham M, *et al*. Organ specific mapping of *in vivo* redox state in control and cigarette smoke-exposed mice using EPR/NMR co-imaging. *J Magn Reson* 2012; **216**: 21–27.
11 Cotrim AP, Hyodo F, Matsumoto KI, *et al*. Differential radiation protection of salivary glands versus tumor by Tempol with accompanying tissue assessment of Tempol by magnetic resonance imaging. *Clin Cancer Res* 2007; **13**: 4928–4933.
12 Hyodo F, Murugesan R, Matsumoto K, *et al*. Monitoring redox-sensitive paramagnetic contrast agent by EPRI, OMRI and MRI. *J Magn Reson* 2008; **190**: 105–112.
13 Halpern HJ. Stable soluble paramagnetic compounds. In: Berliner LJ, ed. *In Vivo EPR (ESR): Theory and Application*. Boston, MA: Springer US, 2003; 201–232.
14 Deguchi H, Yasukawa K, Yamasaki T, *et al*. Nitroxides prevent exacerbation of indomethacin-induced gastric damage in adjuvant arthritis rats. *Free Radic Biol Med* 2011; **51**: 1799–1805.
15 Yasukawa K, Shigemi R, Kanbe T, *et al*. *In vivo* imaging of the intra- and extracellular redox status in rat stomach with indomethacin-induced gastric ulcers using overhauser-enhanced magnetic resonance imaging. *Antioxidants Redox Signal* 2019; **30**: 1147–1161.
16 Pawlak A, Ito R, Fujii H, Hirata H. Simultaneous molecular imaging based on electron paramagnetic resonance of 14N- and 15N-labelled nitroxyl radicals. *Chem Commun (Camb)* 2011; **47**: 3245–3247.
17 Liu Y, Villamena FA, Song Y, Sun J, Rockenbauer A, Zweier JL. Synthesis of 14N- and 15N-labeled trityl-nitroxide biradicals with strong spin-spin interaction and improved sensitivity to redox status and oxygen. *J Org Chem*

*See online. https://doi.org/10.3164/jcbn.20-172

doi: 10.3164/jcbn.20-172

2010; **75**: 7796–7802.
18 Utsumi H, Yamada KI, Ichikawa K, *et al*. Simultaneous molecular imaging of redox reactions monitored by Overhauser-enhanced MRI with ^{N}14- and ^{N}15-labeled nitroxyl radicals. *Proc Natl Acad Sci U S A* 2006; **103**: 1463–1468.
19 Yasukawa K, Hirago A, Yamada K, Tun X, Ohkuma K, Utsumi H. *In vivo* redox imaging of dextran sodium sulfate-induced colitis in mice using Overhauser-enhanced magnetic resonance imaging. *Free Radic Biol Med* 2019; **136**: 1–11.
20 Kosem N, Naganuma T, Ichikawa K, *et al*. Whole-body kinetic image of a redox probe in mice using Overhauser-enhanced MRI. *Free Radic Biol Med* 2012; **53**: 328–336.
21 Benial AMF, Ichikawa K, Murugesan R, Yamada K, Utsumi H. Dynamic nuclear polarization properties of nitroxyl radicals used in Overhauser-enhanced MRI for simultaneous molecular imaging. *J Magn Reson* 2006; **182**: 273–282.
22 Enomoto A, Emoto M, Fujii H, Hirata H. Four-channel surface coil array for sequential CW-EPR image acquisition. *J Magn Reson* 2013; **234**: 21–29.